Air Vehicle Target Recognition with Jammer Nulling Adaptive Waveforms in Cognitive Radar using High-Fidelity RCS Responses

Q. Jeanette O. Tan
Department of Electrical and Computer Engineering
Naval Postgraduate School
Monterey, CA, USA
qtan@nps.edu, tqinling@dso.org.sg

Ric A. Romero
Department of Electrical and Computer Engineering
Naval Postgraduate School
Monterey, CA, USA
rnromero@nps.edu

***Abstract*—In this paper, we introduce two new jammer nulling transmit-adaptive waveforms applied to cognitive radar (CRr) framework for air vehicle (or aircraft) target response recognition in the presence of narrowband jammer noise and AWGN. The jammer nulling adaptive waveforms function as a countermeasure against narrowband jamming signals that disrupts the CRr platform's ability to classify the targets accurately when utilizing jammer-uncompensated adaptive waveforms. The jammer nulling waveforms are derived based on optimizing signal-to-interference-plus-noise-ratio (SINR) and mutual information (MI) metrics; while the adaptive waveforms are obtained by the jammer incorporated probability-weighted energy (PWE) or probability-weighted spectral density (PWSD) method. High-fidelity EM simulated radar cross section (RCS) responses of aircraft targets are utilized to investigate the performance of jammer nulling adaptive waveforms. The results from simulations show an improvement in jamming nulling SINR and MI-based waveforms' classification performance over their jammer-uncompensated counterparts and the receive-adaptive wideband pulsed waveform. The increase in classification performance depends on the target frequency responses and the narrowband jammer spectrum profile.**

***Index Terms*—cognitive radar, waveform design, matched waveform, eigenwaveform, mutual information, target recognition, jammer, electronic warfare, aircraft target**

I. Introduction

Cognitive Radar (CRr) is a knowledge-aided dynamic radar architecture where the operation of the receiver and transmitter are controlled adaptively through provision for feedback about the electromagnetic (EM) environment [1]. Consequently, transmit waveform design using feedback from the CRr interactions with the environment is crucial to a closed-loop system's performance. The use of experience gained through interactions with the EM environment in a CRr framework to maintain stable and reliable operation mirrors the essence of electronic warfare (EW) and the interactions between its subdivisions: electronic support (ES), electronic attack (EA) and electronic protection (EP). ES comprises of tasks that intercept, detect and identify sources of radiated EM energy for the purpose of maintaining spectrum situational awareness; EA involves the use EM energy to disrupt one's ability to utilize the EM spectrum (this includes jamming); and EP protects equipment, capabilities and personnel against EA.

In this paper, we investigate the performance of various transmit-adaptive waveforms used for aircraft target RCS response recognition in CRr in the presence of narrowband jammer (NBJ) interference. This paper's new contribution includes the introduction of new jammer nulling transmit-adaptive waveforms designed to suppress the effects of NBJ on target recognition. Jammer nulling transmit-adaptive waveforms based on signal-to-interference-plus-noise-ratio (SINR) and mutual information (MI) metrics are compared against jammer-uncompensated transmit-adaptive waveforms and receive-adaptive wideband (WI) pulse waveform in terms of the their ability to correctly classify the aircraft in the presence of a NBJ. The adaptive waveform at each closed-loop transmission is obtained by the probability-weighted energy (PWE) or probability-weighted spectral density (PWSD) method that mitigates jammer interference. The jammer nulling adaptive waveforms serve as a countermeasure against NBJ signals that try to disrupt the CRr platform's ability to correctly classify air targets using jammer-uncompensated adaptive waveforms. To ensure the validity of results presented, high-fidelity EM simulated RCS responses of aircraft targets are utilized in the CRr for target response recognition.

Two energy-constrained waveform design approaches that maximize SNR and MI for an extended target in additive Gaussian noise (AWGN) were introduced in [2]. Adaptive waveform design using SNR and MI-based techniques in a CRr framework for target recognition was addressed in [3], [4]. The design of optimal waveform using SNR and MI-based metrics matched to deterministic or stochastic targets in signal-dependent interference and/or AWGN was addressed in [5], [6]. High-fidelity target model signatures were used in [7] and [8] to demonstrate the performance of waveform design in CRr for angle discrimination and target class recognition given aspect angle uncertainty respectively.

This paper is organized as follows. In Section II, we present the signal model utilized in this paper. Section III presents the jammer nulling transmit-adaptive waveform design based on optimizing SINR and MI metrics. Section IV introduces a closed-loop radar framework for target recognition that incorporates and mitigates jamming interference; and presents the probability-weighted waveform update methodologies. Section

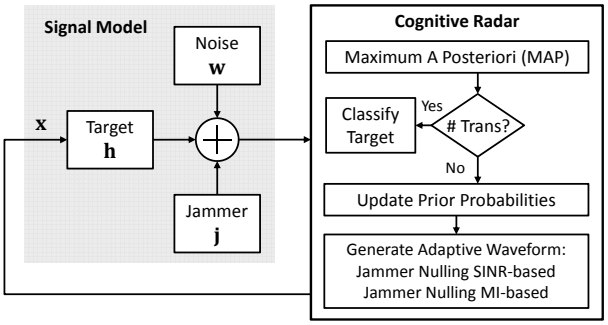

Fig. 1. Block diagram of signal model and cognitive radar platform for target recognition using jammer nulling adaptive matched waveform design.

V describes the generation of practical aircraft target set and their respective high-fidelity EM simulated RCS responses. Section VI presents the target classification results of the narrowband jammer nulling transmit-adaptive waveforms and compares their performance against the uncompensated waveforms. Section VII summarizes and concludes this paper.

II. Signal Model

Figure 1 shows the complex-valued baseband signal model being considered. For brevity, continuous-time passband signals have been downconverted to baseband. As is the convention in signal processing, sampling time is now normalized. Let $x[n]$ be a finite-energy complex-valued transmit waveform vector of length L with discrete Fourier transform (DFT) $X[f]$ where $f = 0, 1/L, 2/L, ..., 1$. Let $h[n]$ represent a deterministic target with discrete Fourier transform $H[f]$. Let $\mathbf{j}[n]$ represent a narrowband jammer with power spectral density (PSD) $S_{jj}[f]$. Let $\mathbf{w}[n]$ be a complex-valued noise from the receiver hardware with PSD $S_{nn}[f]$. The received signal plus jammer interference and noise vector is $\mathbf{y}[n] = s[n] + \mathbf{j}[n] + \mathbf{w}[n]$ where $s[n]$ is the convolution of the transmit waveform and target response ($s[n] = x[n] * h[n]$).

III. Jammer Nulling Waveform Design

We now present jammer nulling transmit-adaptive waveform design approaches that maximize SINR and MI for an extended target.

A. Jammer Nulling SINR-Based Waveform Design

The SINR for a known target is given by

$$\text{SINR} = \sum_f \frac{|H[f]|^2 |X_j[f]|^2}{S_{jj}[f] + S_{nn}[f]} \Delta f, \tag{1}$$

where jammer PSD $S_{jj}[f]$ is incorporated in the SINR expression and $\Delta f = 1/L$.

The finite-duration, energy-constrained jammer nulling waveform $x_j[n]$ that maximizes SINR at the receiver-filter output is obtained from the solution to the Fredholm equation

$$\lambda_{\max} \hat{x}_j[n] = \sum_k \hat{x}_j[n] \hat{R}_{j,h}[n-k], \tag{2}$$

where $\hat{x}_j[n]$ is the maximum eigenvector corresponding to the maximum eigenvalue $\lambda_{\max}$ and $\hat{R}_{j,h}[n]$ is the kernel

$$\hat{R}_{j,h}[n] = \text{IDFT}\left\{ \frac{|H[f]|^2}{L(S_{jj}[f] + S_{nn}[f])} \right\}. \tag{3}$$

A complete vector formulation can be implemented such that the received energy due to the target return is given as

$$E_r = E_x E_h \bar{\mathbf{x}}_j^\dagger \bar{\mathbf{H}}^\dagger \mathbf{R}_{jn}^{-1} \bar{\mathbf{H}} \bar{\mathbf{x}}_j = E_x E_h \bar{\mathbf{x}}_j^\dagger \bar{\mathbf{R}}_T \bar{\mathbf{x}}_j, \tag{4}$$

where $\mathbf{h} = \sqrt{E_h}\bar{\mathbf{h}}$ such that E_h is the target response energy and $\bar{\mathbf{h}}$ is the corresponding unit energy vector; $\mathbf{x}_j = \sqrt{E_x}\bar{\mathbf{x}}_j$ where E_x is the transmit waveform energy and $\bar{\mathbf{x}}_j$ is the unit energy vector. The total autocorrelation $\bar{\mathbf{R}}_T$ is a function of the target convolution matrix $\bar{\mathbf{H}}$ and interference-plus-noise autocorrelation $\bar{\mathbf{R}}_{jn} = \bar{\mathbf{R}}_j + \bar{\mathbf{R}}_n$.

The jammer nulling matched transmit waveform based on maximizing SINR criterion in (1) is obtained by performing eigenvalue-decomposition of (4) to derive the eigenwaveform corresponding to the maximum eigenvalue

$$E_{r,\lambda_{\max}} = E_x E_h \bar{\mathbf{q}}_{\max}^\dagger \lambda_{\max} \bar{\mathbf{q}}_{\max}, \tag{5}$$

where $E_{r,\lambda_{\max}}$ is the received energy, $\bar{\mathbf{q}}_{\max}$ is the eigenwaveform corresponding to the maximum eigenvalue $\lambda_{\max}$. The jammer nulling matched transmit waveform that maximizes the received return energy is expressed as a function of the eigenwaveform as $\bar{\mathbf{x}}_j = \bar{\mathbf{q}}_{\max}$.

The uncompensated SNR-based transmit-adaptive waveform can easily be calculated by setting $S_{jj}[f] = 0$ and maximizing the metric in (1).

B. Jammer Nulling MI-Based Waveform Design

The MI between an ensemble of Gaussian targets and the received signal in the presence of jammer interference and AWGN is

$$I_j(\mathbf{y}; \mathbf{h}|\mathbf{x}) = \sum_f \ln \left[1 + \frac{|X[f]|^2 \sigma_H^2[f]}{L(S_{jj}[f] + S_{nn}[f])} \right] \Delta f, \tag{6}$$

where $\mathbf{y}$ is the receiver output signal, $\mathbf{h}$ is the stochastic target impulse response, $\mathbf{x}$ is the transmit waveform with length L and $S_{jj}[f]$ is the jammer interference PSD.

The jammer nulling waveform that optimizes MI in (6) with respect to $|X_j[f]|^2$ is given by a waterfilling waveform

$$|X_j[f]|^2 = \max\left[0, A - \frac{L(S_{jj}[f] + S_{nn}[f])}{\sigma_H^2[f]} \right], \tag{7}$$

where $|X_j[f]|^2$ is the energy spectral density (ESD) of the jammer nulling transmit waveform $x_j[n]$, $\sigma_H^2[f]$ is the energy spectral variance (ESV) of length L and $S_{nn}[f]$ is the receiver noise PSD.

The water-level A is determined by the following energy constraint

$$\sum_f \max\left[0, A - \frac{L(S_{jj}[f] + S_{nn}[f])}{\sigma_H^2[f]} \right] \Delta f \leq E_x, \tag{8}$$

where A can be found by simple methods such as the bisection

algorithm.

The uncompensated MI-based transmit-adaptive waveform is obtained by optimizing the MI metric in (6) with $S_{jj}[f] = 0$.

IV. Closed-Loop Radar Platform for Aircraft Target Response Recognition

Figure 1 shows the application of jammer nulling adaptive matched waveform design in CRr for target recognition in the presence of jammer interference. We fix the number of transmissions and maximum a posteriori (MAP) is used to determine the target decision based on the most likely hypothesis after the last waveform transmission.

Consider a target recognition problem where one of the M possible targets is present. This results in a multiple hypothesis testing (MHT) problem where the i^{th} hypothesis is characterized by the target response $\mathbf{h}_i$ and its convolution matrix $\bar{\mathbf{H}}_i$ where $i = 1, 2, ..., M$. A Bayesian representation of the channel is formulated where the target hypotheses are denoted by $\mathcal{H}_1, \mathcal{H}_2, ..., \mathcal{H}_M$ with corresponding prior probabilities $P_1, P_2, ..., P_M$. In discrete-time implementation, the i^{th} hypothesis is expressed as

$$\mathcal{H}_i : \mathbf{y} = \mathbf{s}_i + \mathbf{j} + \mathbf{w} = \mathbf{h}_i * \mathbf{x} + \mathbf{j} + \mathbf{w} = \sqrt{E_h}\bar{\mathbf{H}}_i\sqrt{E_x}\bar{\mathbf{x}}_i + \mathbf{j} + \mathbf{w}, \tag{9}$$

where $\mathbf{h}_i$ is the i^{th} target impulse response.

With jammer noise $\mathbf{j} \sim \mathcal{CN}(0, \mathbf{R}_j)$ and AWGN $\mathbf{w} \sim \mathcal{CN}(0, \sigma^2\mathbf{I})$, the corresponding pdfs are

$$p(\mathbf{y}|\mathcal{H}_i) = \frac{1}{\pi^{L_y}\det(\mathbf{C}_{jn})}\exp\left[-(\mathbf{y}-\mathbf{s}_i)^\dagger \mathbf{C}_{jn}^{-1}(\mathbf{y}-\mathbf{s}_i)\right], \tag{10}$$

where $\mathbf{C}_{jn} = \mathbf{R}_{jn} = \mathbf{R}_j + \sigma^2\mathbf{I}$ and L_y is the length of $\mathbf{y}$.

In a CRr framework that utilizes adaptive waveform design, the jammer nulling matched waveform for each target hypothesis is derived by optimizing SINR or MI-based metrics. The transmit waveform is obtained by scaling each target's optimum waveform with its corresponding hypothesis probability from (10) using the PWE or PWSD method.

For the PWE method, each matched waveform corresponding to a target hypothesis is scaled by its updated probability as given by

$$\mathbf{x}_{\text{pwe}} = \sum_{i=1}^{M}\sqrt{P_i}\bar{\mathbf{q}}_{i,\max}, \tag{11}$$

and transmit energy constraint is simply accommodated by

$$\mathbf{x} = \sqrt{E_x}\frac{\mathbf{x}_{\text{pwe}}}{\sqrt{E_{x_{\text{pwe}}}}}. \tag{12}$$

For deterministic targets, the PWSD for all hypotheses is

$$|H(f)|^2 = \sum_{i=1}^{M} Pr(\mathcal{H}_i)|H_i(f)|^2 - \left|\sum_{i=1}^{M} Pr(\mathcal{H}_i)\sqrt{|H_i(f)|^2}\right|^2. \tag{13}$$

where $Pr(\mathcal{H}_i)$ is the probability that the i^{th} hypothesis is true and $|H_i(f)|^2$ is the i^{th} target ESD.

The PWSD function in (13) is used in place of target ESV in (7) to derive the matched jammer nulling waveforms based on MI criterion.

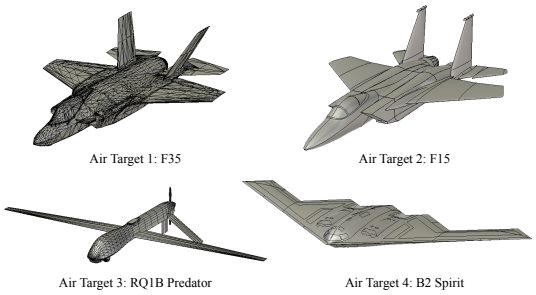

Fig. 2. Aircraft target CAD models.

The closed-loop radar system retains information and knowledge obtained through previous received signals and iterations using a Bayesian probability update rule for the i^{th} target at $(k+1)^{\text{th}}$ iteration

$$P_{i,(k+1)} = \beta p(\mathbf{y}_{(k+1)}|\mathcal{H}_i)P_{i,(k)}, \tag{14}$$

where $p(\mathbf{y}_{(k)}|\mathcal{H}_i)$ is the measurement pdf after the k^{th} iteration and β ensures unit total probability over the target classes at each iteration.

V. Aircraft Target Set

In this paper, a set of four publicly available aircraft Computer-Aided Design (CAD) models shown in Figure 2 are modified to actual scale and size. The publicly available CAD models are either cost free or for a fee. These models are imported to Computer Simulation Technology (CST) Microwave Studio (MWS) simulation software. The asymptotic solver that utilizes the ray tracing technique is used to generate high-fidelity EM-simulated frequency responses at head-on angle of incidence, i.e. 0° in azimuth ($\theta_{az} = 0^\circ$) and 0° degree in elevation ($\theta_{el} = 0^\circ$). Airborne EW receivers, like the radar warning receiver (RWR) typically operate in the 0.5 to 18 GHz frequency range with airborne intercept applications operating in the X-band (8 to 12 GHz). Hence, in this paper we consider aircraft target frequency responses between 9 to 10 GHz. The 9 to 10 GHz magnitude frequency responses based on RCS responses generated in CST are shown in Figure 3. The frequency responses are wideband and contain rich frequency components, making the wideband impulse waveform a good candidate waveform for all the targets. Indeed, it will be used as a benchmark to compare with adaptive waveforms. These passband frequency responses are downconverted to normalized baseband impulse responses in Figure 4. The aircraft target impulse responses (real part) consist of delta-like functions and appear slightly correlated due to physical similarities between aircrafts.

VI. Results

We now present the performance results of CRr utilizing transmit-adaptive waveforms for aircraft target recognition. The number of transmissions by the closed-loop system is parameterized and MAP detection rule is used to classify the target. The target with the highest hypothesis probability is selected as the system's decision. Percentage of

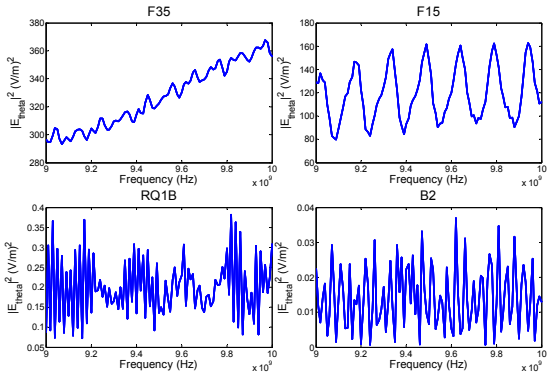

Fig. 3. Aircraft target 9-10 GHz magnitude frequency responses at $\theta_{az} = 0°$ and $\theta_{el} = 0°$.

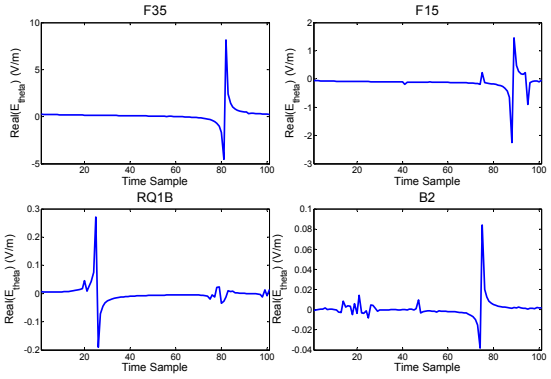

Fig. 4. Aircraft target 9-10 GHz impulse responses (real part) at $\theta_{az} = 0°$ and $\theta_{el} = 0°$.

correct classification (P_{cd}) is used as a metric to quantify and compare jammer nulling adaptive waveform performance. The jammer nulling waveforms considered are: a) jammer nulling SINR-based probability-weighted energy waveform (JN-SINR-PWE), b) jammer nulling MI-based probability-weighted energy waveform (JN-MI-PWE), and c) jammer nulling MI-based probability-weighted spectral density waveform (JN-MI-PWSD). The classification performance of these jammer nulling waveforms are compared against their uncompensated counterparts and the receiver-adaptive wideband pulsed waveform, i.e. SNR-PWE, MI-PWE, MI-PWSD and WI.

The impulse responses corresponding to the target aircrafts shown in Figure 4 are used in the experiments to generate P_{cd} against transmit waveform energy E_x over $100,000$ Monte Carlo simulations. Single and multiple transmissions are considered where the number of transmissions are $\#\text{Tx} = 1, 2, 4, 10$. Here, we will present the following results: classification performance of the uncompensated adaptive waveforms in the presence of NBJ interference and AWGN; and classification performance of jammer nulling adaptive waveforms in the presence of NBJ interference and AWGN. The aircraft target recognition performance gain of jammer nulling waveforms over uncompensated waveforms with 9.4-9.6 GHz NBJ or 9.8-10 GHz NBJ interference is also examined.

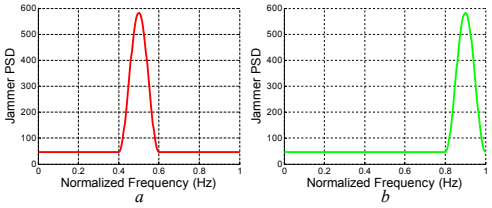

Fig. 5. NBJ noise PSD normalized in frequency corresponding to 9-10 GHz with JNR=20dB and AWGN set at 1W. a) NBJ-1, b) NBJ-2.

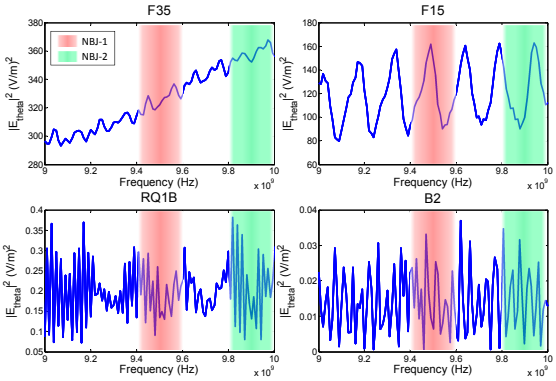

Fig. 6. Aircraft target 9-10 GHz magnitude frequency responses with a narrowband jammers NBJ-1 and NBJ-2.

A. Aircraft Target Response Recognition with Jammer-Uncompensated Adaptive Waveforms in NBJ Noise

Now we present the classification performance results for uncompensated and jammer nulling adaptive waveforms in CRr in the presence of NBJ noise and AWGN. Here we consider two arbitrarily generated NBJ noise: NBJ-1 with bandwidth from 9.4-9.6 GHz and NBJ-2 with bandwidth from 9.8-10 GHz with jammer-to-noise ratio JNR = 20 dB and PSD $S_{jj}[f]$ shown in Figure 5. The target response frequencies affected by the respective NBJs are illustrated in Figure 6.

The classification performance of uncompensated WI, SNR-PWE, MI-PWE and MI-PWSD adaptive waveforms in the presence of NBJ-1 and NBJ-2 are shown in Figure 7 and 8 respectively. Referring to Figure 7, the performance gain of transmit-adaptive waveforms over the WI waveform is more pronounced in this case with SNR-PWE achieving the best performance with a single transmission and MI-PWSD achieving improved P_{cd} with greater number of transmissions. With high frequency NBJ-2, the target recognition performance in Figure 8 shows that P_{cd} of transmit-adaptive waveforms are significantly affected. The performance of the MI-PWE waveform is the best amongst all transmit-adaptive waveforms, achieving comparable P_{cd} to that from the WI waveform. Interestingly, WI waveform outperforms the transmit-adaptive SNR-PWE and MI-PWSD in this case. The relative performance of transmit-adaptive waveforms compared to the receive-adaptive WI waveform differs due to target response frequency components affected by the NBJ. Referring to Figure 6, although all the targets are generally wideband, the magnitude frequency responses are slightly greater in 9.8-10 GHz frequency band

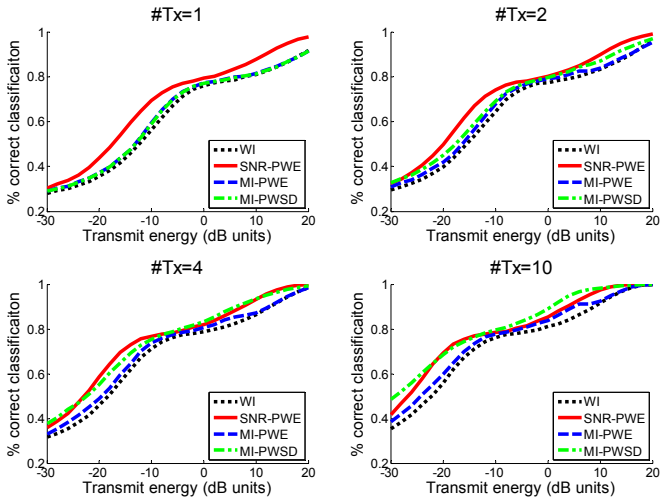

Fig. 7. Classification performance for uncompensated WI, SNR-PWE, MI-PWE and MI-PWSD adaptive waveforms in NBJ-1 noise and AWGN.

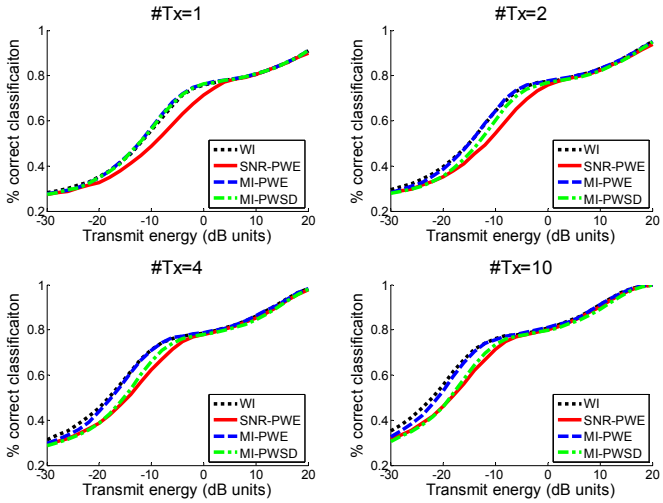

Fig. 8. Classification performance for uncompensated WI, SNR-PWE, MI-PWE and MI-PWSD adaptive waveforms in NBJ-2 noise and AWGN.

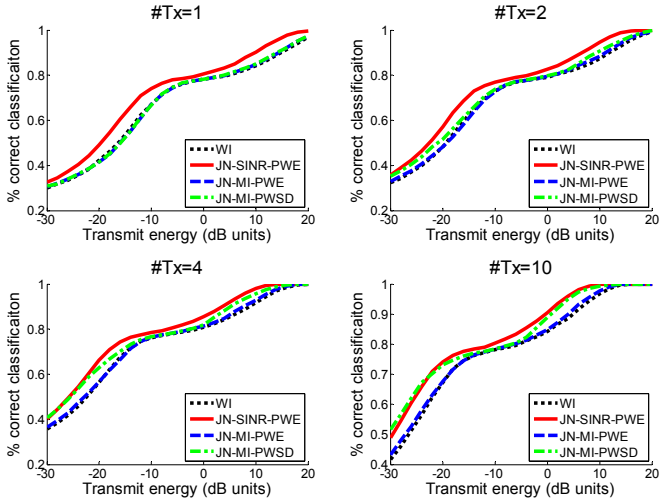

Fig. 9. Classification performance for jammer nulling adaptive waveforms WI, JN-SINR-PWE, JN-MI-PWE and JN-MI-PWSD in NBJ-1 noise and AWGN.

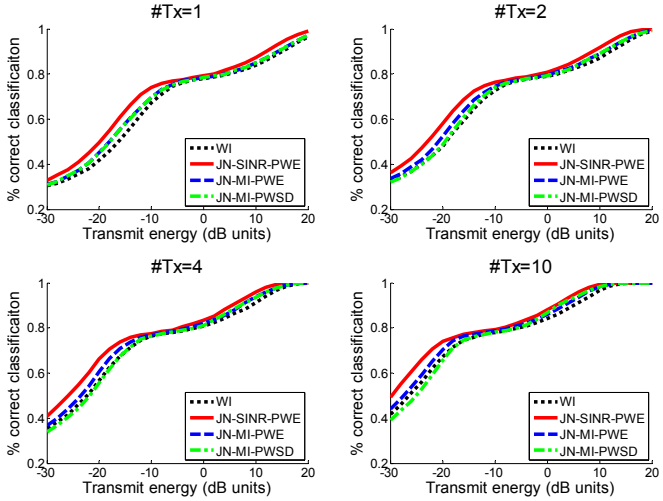

Fig. 10. Classification performance for jammer nulling adaptive waveforms WI, JN-SINR-PWE, JN-MI-PWE and JN-MI-PWSD in NBJ-2 noise and AWGN.

compared to the 9.4-9.6 GHz band for the F35 and RQ-1B. Introducing a NBJ in the 9.8-10 GHz frequency band will therefore impact the classification performance of transmit-adaptive waveforms more significantly.

B. Aircraft Target Response Recognition with Jammer Nulling Adaptive Waveforms in NBJ Noise

The classification performance of jammer nulling adaptive waveforms JN-SINR-PWE, JN-MI-PWE and JN-MI-PWSD in the presence of NBJ-1 and NBJ-2 are shown in Figure 9 and 10 respectively. With NBJ-1 and AWGN (Figure 9), the JN-SINR-PWE waveform achieves the best P_{cd} with single transmission, with a 3 dB performance gain over the WI waveform at $P_{cd} = 0.70$. With multiple transmissions, the JN-SINR-PWE is generally the best performer, maintaining a 3-4 dB performance gain over WI waveform at $P_{cd} = 0.70$. Although the performance of JN-MI-PWE and JN-MI-PWSD is marginally better than the WI with a single transmission, its P_{cd} improves with the number of transmissions. The improvement of classification performance with number of transmissions is more pronounced for the JN-MI-PWSD waveform. With 10 transmissions, the JN-MI-PWSD waveform P_{cd} approaches that of the JN-SINR-PWE for certain transmit energy levels. Likewise, with NBJ-2 and AWGN (Figure 10), the JN-SINR-PWE waveform is the best performer with single and multiple transmissions, achieving a 4 dB performance gain over the WI waveform at $P_{cd} = 0.70$. The classification performance of the JN-MI-PWE and JN-MI-PWSD is marginally better than the WI waveform for a single transmission with the JN-MI-PWE maintaining its performance gain over the WI waveform as the number of transmissions increases. The JN-MI-PWSD however, loses its performance gain over the WI as the number of transmissions increases.

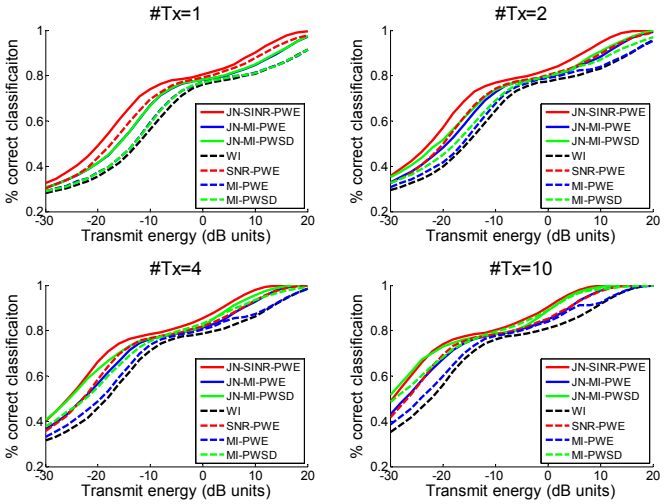

Fig. 11. Classification performance comparison for JN-SINR-PWE, JN-MI-PWE and JN-MI-PWSD adaptive waveforms with uncompensated counterparts in the presence of NBJ-1 noise and AWGN.

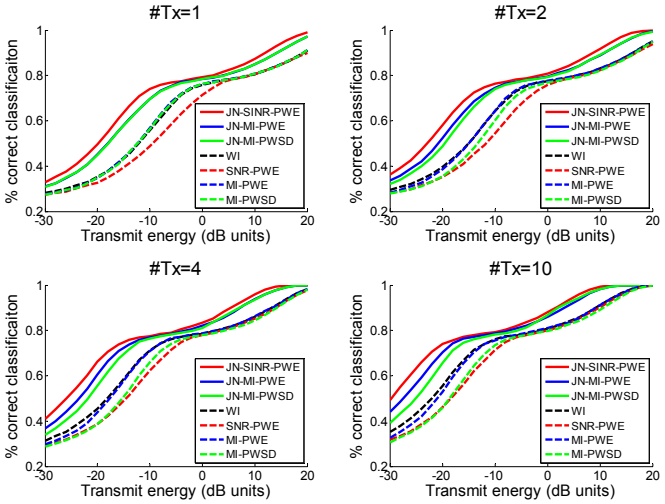

Fig. 12. Classification performance comparison for JN-SINR-PWE, JN-MI-PWE and JN-MI-PWSD adaptive waveforms with uncompensated counterparts in the presence of NBJ-2 noise and AWGN.

The performance curves for the jammer nulling adaptive waveforms and the uncompensated adaptive waveforms with NBJ-1 noise and AWGN in Figure 7 and Figure 9 are shown together in Figure 11 to facilitate comparison. The transmit-adaptive JN-SINR-PWE, JN-MI-PWE, JN-MI-PWSD and the uncompensated SNR-PWE, MI-PWE, MI-PWSD generally perform better than the WI waveform in the presence of NBJ-1 noise and AWGN. The JN-SINR-PWE achieves the best classification performance for a single transmission. For multiple transmissions, JN-SINR-PWE is one of the best performers, followed closely by the JN-MI-PWSD. It is worth noting that for a single transmission, the uncompensated SNR-PWE achieves a slightly better P_{cd} than the JN-MI-PWE and JN-MI-PWSD. Nevertheless, the P_{cd} of the JN-MI-PWSD improves with the number of transmissions. With 2 transmissions, the JN-MI-PWSD performance matches that of the uncompensated SNR-PWE; and with 4 transmissions the JN-MI-PWSD P_{cd} exceeds that of the uncompensated SNR-PWE at most transmit energy levels. Similarly, the performance of the JN-MI-PWE improves with the number of transmission; by 10 transmissions, the JN-MI-PWE achieves a similar P_{cd} as the uncompensated SNR-PWE.

Likewise, the performance profiles for the jammer nulling adaptive waveforms and the uncompensated adaptive waveforms with NBJ-2 noise and AWGN in Figure 8 and Figure 10 are shown together in Figure 12 for easy comparison. The improvement in classification performance of jamming nulling adaptive waveforms over their uncompensated counterparts is more pronounced in the presence of high frequency NBJ-2 noise that affects significant target response frequency components. The JN-SINR-PWE achieves the best classification performance for single and multiple transmissions, followed by the JN-MI-PWE and JI-MI-PWSD. Unlike the previous case where NBJ-1 is present, all jammer nulling adaptive waveforms perform better than the uncompensated counterparts in the presence of NBJ-2 noise.

VII. Summary and Conclusion

In this paper, we introduced new jammer nulling transmit-adaptive waveforms that optimize SINR and MI metrics for aircraft recognition on a CRr platform. High-fidelity aircraft target frequency responses were generated in CST using CAD models. We examined the performance gain of jammer nulling transmit-adaptive waveforms in CRr over their uncompensated counterparts and the receive-adaptive WI pulsed waveform for single and multiple transmissions. The results from simulations show that there is moderate to significant improvement for the jammer nulling JN-SINR-PWE waveform over the uncompensated waveforms and receive-adaptive WI waveform. The extent of improvement in classification performance depends on target frequency responses and the NBJ frequency profile.

References

[1] S. Haykin, "Cognitive radar: A way of the future," *IEEE Signal Process. Mag.*, vol. 23, no. 1, pp.30-40, Jan. 2006.

[2] M. R. Bell, "Information theory and radar waveform design," *IEEE Trans. Inform. Theory*, vol. 39, no. 5, pp.1578-1597, Sep. 1993.

[3] N. A. Goodman, P. R. Venkata and M. A. Neifeld, "Adaptive waveform design and sequential hypothesis testing for target recognition with active sensors," *IEEE J. of Sel. Topics in Sig. Proc. Mag.*, vol. 1, no. 1, pp.105-113, Jun. 2007.

[4] R. A. Romero and N. A. Goodman, "Improved waveform design for target recognition with multiple transmissions," *2009 Int. Waveform Diversity and Design Conf.*, pp.26-30, 2009.

[5] R. A. Romero, J. Bae and N. A. Goodman, "Theory and application of SNR and mutual information matched illumination waveforms," *IEEE Trans. Aero. and Elec. Sys.*, vol. 47, no. 2, pp.912-926, Apr. 2011.

[6] A. Aubry *et al.*, "Knowledge-aided (potentially cognitive) transmit signal and receive filter design in signal-dependent clutter," *2013 IEEE Trans. Aero. and Elec. Sys.*, vol. 49, no. 1, pp.93-117, Jan 2013.

[7] J. Bae and N. A. Goodman, "Automatic target recognition with unknown orientation and adaptive waveforms," *2011 IEEE Radar Conf.*, pp.1000-1005, May 2011.

[8] Q. J. O. Tan, R. A. Romero and D. C. Jenn, "Target recognition with adaptive waveforms in cognitive radar using practical target RCS responses," *2018 IEEE Radar Conf.*, 2018.